

Multi-spectral Infrared Computed Tomography

Philip Bingham, Marissa E. Morales-Rodriguez, Panos Datskos, and David Graham
Oak Ridge National Laboratory, Oak Ridge, TN

Abstract

Precise measurement of spatial gas concentrations in an uncontrolled outdoor environment is needed for environmental studies. In this effort, a multispectral imaging system has been developed incorporating quantum cascade laser (QCL) modules with an iterative computed tomography algorithm to sense a transmission spectrum response for each voxel. With spatially distributed spectral data, researchers will be able to identify gas composition and concentration distributions over a region of interest. The QCL system uses multiple modules covering wavelength ranges from $3.77\mu\text{m}$ to $12.5\mu\text{m}$ to detect both carbon dioxide ($4.2\mu\text{m}$) and methane ($7.5\mu\text{m}$) greenhouse gasses. Simulation and lab studies have been performed for a system using a circular arrangement of mirrors to transmit and reproject the QCL beam around the detector circle. The QCL transmission system has been tested in both controlled indoor environments and uncontrolled outdoor environments to quantify sensitivity.

Notice: This manuscript has been authored by UT-Battelle, LLC, under Contract No. DE-AC0500OR22725 with the U.S. Department of Energy. The United States Government retains and the publisher, by accepting the article for publication, acknowledges that the United States Government retains a non-exclusive, paid-up, irrevocable, world-wide license to publish or reproduce the published form of this manuscript, or allow others to do so, for the United States Government purposes. The Department of Energy will provide public access to these results of federally sponsored research in accordance with the DOE Public Access Plan (<http://energy.gov/downloads/doe-public-access-plan>).

Introduction

Arctic tundra is rapidly evolving as permafrost degrades, exposing vast amounts of stored carbon to degradation that could produce a mixture of greenhouse gasses (GHGs). Ecosystem experiments are underway to answer fundamental questions regarding the feedback from high-latitude warming on the global climate system [1]. In order to parameterize and test a process-rich ecosystem model at plot scales of tens to hundreds of meters, monitoring the chemical environment over such a large scale is important. Chemical species such as CO_2 , CH_4 , H_2O and, perhaps, N_2O need to be monitored as a function of time in terms of quantity and location. Experiments designed to quantify the physical, chemical, and biological behavior of terrestrial ecosystems require methods for measurement of gas distributions across the ecosystem under study. Currently these measurements are made with single point measurement systems using soil gas flux chambers, plot-scale measurements integrated across a flux footprint of a tower-mounted eddy covariance system, or via periodic airborne measurements[2][3].

In this work, a method for the measurement of the spatial distribution of GHG emissions across the region under study is being developed using multi-spectral computed tomography in the mid-infrared (mid-IR) band. The goal is to eventually provide an efficient, deployable system that will provide persistent spatial information about gasses present, their identities and

concentrations over large areas ($>1\text{km}^2$). In the following sections, the IR computed tomography (IR-CT) system that has been developed is described along with an iterative CT algorithm implementation with simulation results, and a laboratory measurement is presented.

System Design

A conceptual drawing for a field-based IR computed tomography (IRCT) system is shown in Figure 1. This design uses a single source containing four pulsed broadly tunable external cavity quantum cascade laser (QCL) modules [4][5][6] that produce a wavelength range from $3.77\mu\text{m}$ to $12.5\mu\text{m}$ with a spectral resolution of 0.7 to 2nm, depending on the module. Illumination in the mid-IR range is suited for measurements over large outdoor areas since mid-IR lasers remain eye-safe at energy levels high enough to measure over long distances, and the mid-IR band is also less attenuated by moisture in the air than short wavelength IR bands. In this conceptual system, an array of detectors and/or mirrors is located around the region to be scanned. Rotation of the QCL source produces a single projection from the source position as shown by the black arrows in the figure. Depending on cost and implementation constraints, there are a number of methods for producing the additional projections (increasing the number of sources, movement of source around the region of interest, rotational motion of mirrors, etc.). In the drawing, a mirror orientation concept is presented where the source is aimed at a single mirror and the orientation of this mirror in conjunction with the others provides a new projection from that mirror's perspective as shown by the gray arrows.

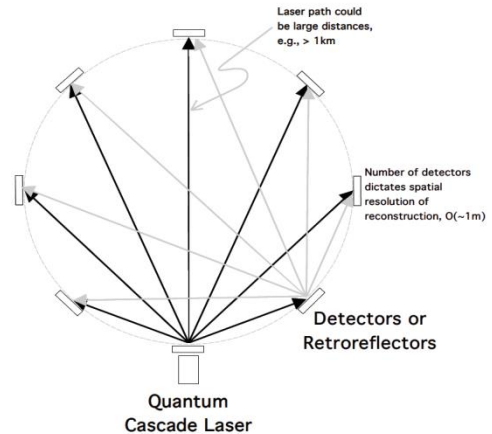


Figure 1. Conceptual system for tomographic measurements in the field.

Figure 2 shows an implementation of the source/detector system developed for outdoor testing. This unit is intended to be used in reflection mode. A mirror-based telescope optic collects the return beam and focuses onto a MCT detector from VIGO systems model PCI-3TE. The MCT detector is a compact three-stage thermoelectrically cooled detector optimized to provide high

performance in the spectral range from 2 to 13 μ m with a specific detectivity (D^*) greater than or equal to 4.5×10^8 cmHz^{1/2}/W. The QCL source module is broadly tunable, pulsed (Uber-Tuner Daylight Solutions, CA) and provides a wavelength range from 7.38 to 8.0 μ m at a peak power of approximately 400mW, for the detection of CH₄. The QCL module is operated in a pulsed mode of 500ns, 100kHz repetition rate, 5% duty cycle and a scan speed of 0.5 μ m/sec. A LabVIEW interface communicates with the QCL module to control the start/stop of the wavelength scan, data collection, display and storage. The data is collected using the multifunctional data acquisition NI USB-6251 BNC from National Instruments. As the QCL module is tuning wavelengths, the LabVIEW interface collects the output voltage from the detector as a function of time. The output voltage of the detector is directly related to the amplitude or intensity of the QCL source per wavelength. LabVIEW uses the Fourier transform to extract the spectral information from the data collected as a function of time.

In the system, the QCL source is reflected off of the reflective pyramid seen in the center of the telescope to place the source in line with the detection pathway. This module also contains a visible laser that is reflected off of the pyramid to aid in alignment of the system. Finally, the entire unit sits on a rotational stage to provide scanning to capture the projection array.

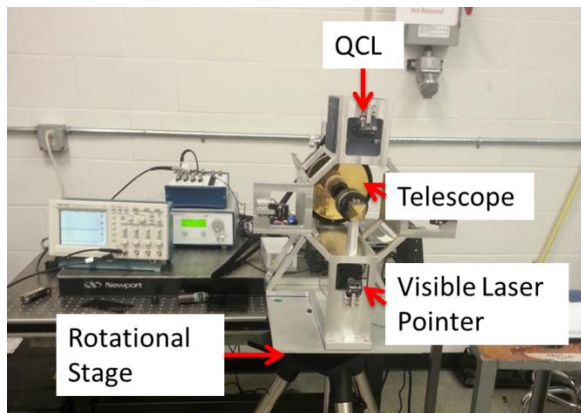


Figure 2. QCL source and telescope based detector module.

Reconstruction Algorithm

Tunable Diode Laser Absorption Spectroscopy (TDLAS) is a similar measurement method to our system. The only difference is the broad range of wavelengths provided by the QCL modules that are used. Computed tomography techniques have been applied to TDLAS in the past. In [7], Hartl provides a study of multiple reconstruction methods applied to a very small number of projections (four or less) with a focus on systems with a limited number of Gaussian shaped gas plumes. Fischer [8] shows a reconstruction of indoor gas distribution using a unique geometry defined by an array of detector/source pairs. This geometry is very close to four parallel projections through the room. The reconstruction is a fit of five Gaussian peaks to the distribution and uses an Algebraic Reconstruction Technique (ART) step for initial peak localization and sizing followed by a simulated annealing step for peak shape refinement. The land areas under study in the Arctic contain irregular-shaped polygonal tundra and thaw lakes resulting from the freeze and thaw cycles. As a result, the gas distributions to be measured are expected to contain shapes related to these landscape features that may not be represented well by Gaussian peaks. In [9], an effort is underway to measure CH₄ over

large areas using two laser wavelengths in ratio. This system scans across an array of retroreflectors and multiple projections are captured by multiple sources positioned around the field. The main differences between this work and our system are use of the QCL to enable measurement of multiple gas concentrations with a high resolution spectrum, and the use of source reprojection to obtain additional projections without the added cost of additional QCLs.

A general reconstruction method has been developed for this proof-of-principle in which a Maximum Likelihood Estimation Method (MLEM)[10] has been modified based on the assumption of smoothness in the gas distribution. Challenges for computed tomographic reconstruction from the multispectral measurements captured with this system come from the unique spacing of detectors around a circle, limitations in measurements providing a limited number of low resolution projections, and unique measurement paths due to reprojection of the source to each mirror for additional projection data. Simulated data was produced for the initial algorithm development through modification of the TAKE code [11]. This code is a ray trace based simulation code for X-ray CT applications. Minor modifications to the “cylinder around rotation axis” detector type were made to incorporate the source into the circle. In this simulation code, basic geometric shapes can be used to define a voxel map for the object under test. For testing, a gas distribution was defined using concentric circles to create two flat top objects with a roll-off to zero. One object had an attenuation of 0.6 on the flat top and the second 0.3. In addition to providing projection sinograms, the TAKE code will also produce an image of the voxel space for requested voxel sizes. In Figure 3, two voxel maps are presented from the code. The left shows a 41 x 41 voxelization of the simulated objects. This resolution is high enough to provide a visual ground truth for the objects. In the simulation, the system consisted of nine mirrors around the circular region, resulting in 10 projections through the space. Calculations of the heat map for number of rays intersecting each voxel indicates that an odd number of detectors gives a more uniform distribution of representation, and the diameter of the area in the detection circle should be no larger than 11 voxels for this setup. Therefore, the expected reconstruction results from the simulated data should match the 11 x 11 voxel map shown on the right in Figure 3.

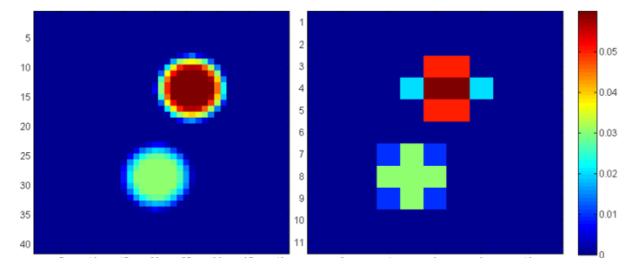


Figure 3. Image of simulated voxel space (left) 41x41 voxels (right) 11 x 11 voxels.

Figure 4 shows two results of 11 x 11 voxel reconstructions. The left image is a reconstruction result from direct application of the MLEM model [10] using simulated data of 10 projections and a system model including the additional rays to reproject the source around the circle. Comparing to the right image in Figure 3, the result appears to have similar cross section values in the correct places with the shapes having some skew. This skew is a result of the few number of projections and uneven sampling of voxels in the projection geometry.

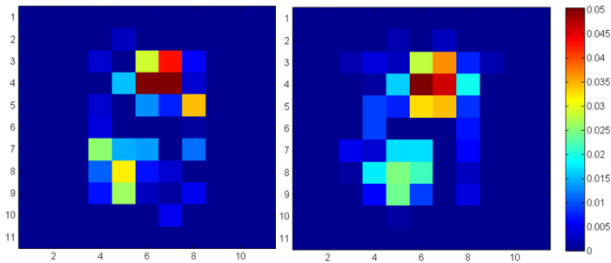


Figure 4. MLEM reconstructions with 11x11 voxel space. (left) MLEM (right) MLEM with projection subsampling

Using the knowledge that the gases will not have sharp gradients in concentration, the first modification for the reconstruction technique was to use interpolation to increase the number of pixels in each projection. This interpolation increased the size of each of the 10 projections from 9 to 49 pixels by interpolating five pixel positions between each pixel in the projection. Linear interpolation between two pixels based on angular distance was implemented. In this circular geometry, the cord through the circle that represents the distance between source and detector varies quickly as the detectors approach the source around the circle. To account for the path length change in the projection interpolation, pixel values of attenuation on either side of the pixel to be interpolated were normalized by the path length for those rays. Interpolation was then performed to get a normalized attenuation value that was multiplied by the source to detector path length associated with the interpolated pixel's location. Reconstruction results from the interpolated projection set are depicted on the right side of Figure 4, and they begin to show shapes more representative of the simulated shapes. Extending the interpolation to increase projection sizes from 49 to 89 pixels and increasing the voxel resolution to 51 x 51 voxels results in the reconstruction presented on the left side of Figure 5. As depicted, the two objects are more clearly separated with defined shapes that have streak artifacts from the low number of projections; also, the peak values on each object are at the proper values. Strong gradients between neighboring voxels violate the assumption of a smooth gas distribution. To account for this, a smooth distribution is forced in the voxel space by use of a mean filter that is employed during each iteration of the reconstruction. With a 3 x 3 mean filter applied to the voxel space, the reconstruction shown on the left side of Figure 5 becomes that depicted on the right. As expected, the result is two circular regions with proper values relative to one another, but with an altered scale.

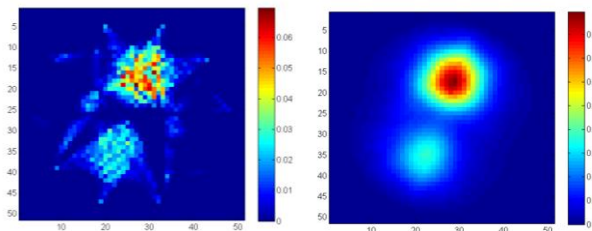


Figure 5. (left) 10 interpolated pixels between each measured pixel (right) same projections smoothing applied in voxel space.

Testing

With the goal of providing a proof-of-principle using the QCL system in conjunction with CT reconstruction, an imaging system was set up on an optical bench, as depicted in Figure 6. The setup entailed an array of 11 mirrors around a 48-inch diameter circle.

For this smaller scale setup, a few modifications in the system geometry were made for ease of setup. To ease the rotational motion requirements for the source, a mirror was used for the source spot and the detector was offset from the source location. In this configuration, only the mirror is required to be placed on the rotational stage. As a result, the QCL was aimed at the source mirror causing an additional path through the area that is included in every projected ray. To ease control requirements on the additional mirrors used for reprojection of the source, we moved the object in a circular rotation within the system to provide rotated projections.

Figure 7 contains a drawing of the lab setup. The QCL was placed next to the source mirror such that it required two rays to pass through the detection area. Rays in this drawing show all the paths associated with measurement of a single projection. The ray between the QCL and the periscope was close to the table but below the measurement plane by approximately six inches and the periscope returned a ray in the measurement plane back to the source mirror. Rotation of the source mirror selected a mirror for measurement and each of those mirrors was positioned to return the light to the detector location. The separation of the source location and the detector resulted in a more complex ray path as the transmitted and reflected rays were not collinear.

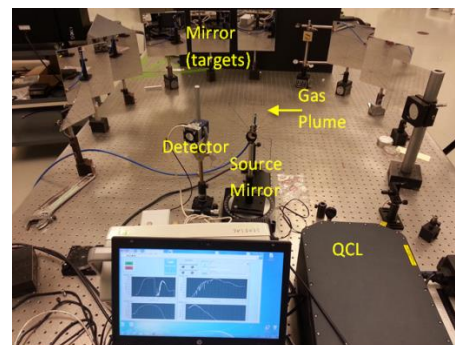


Figure 6. Test system setup

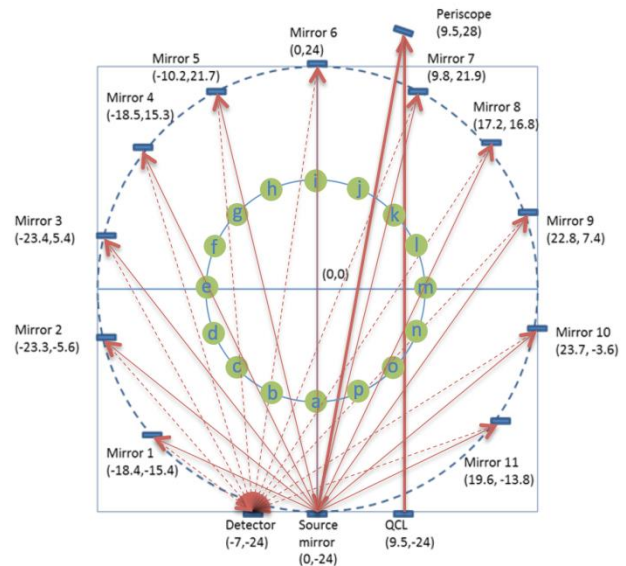


Figure 7. Test setup layout with gas supply locations.

For the lab test, a small tube connected to a gas cylinder containing a concentration of 5% methane was used to provide the

test sample. The tube was placed just below the measurement plane to provide a plume of gas in the plane. Instead of rotating the measurement system around the plume, projections were captured by moving the plume in a circular pattern represented by the dots on the inner circle, which is 24-inches diameter. 16 projections were captured in this manner with 11 mirrors providing 11 pixels per projection. The four-module QCL system is able to scan the laser, collect, display and record data at a rate of 45 seconds per scan for a single mirror. The spectral information of the 6.87-8.52 μm QCL module, corresponding to the CH_4 absorption region, was used for the reported experiment. Each measured ray through the system was captured at 808 equally-spaced wavelengths (2nm steps) within the range resulting in a transmittance plot like the one presented in Figure 8. This plot shows data from a measurement using mirror 6 with the gas plume located in position "a", the closest position to the source mirror. Transmittance was normalized using a projection captured with the gas plume off to remove intensity variations across the wavelengths and any noise resulting from the optics and mirrors. The large attenuation between 7.5 and 7.6 μm corresponds to the methane absorption peak.

Using spectral data for each projection pixel, a reconstruction was performed for each 2nm wavelength bin using the previously described reconstruction algorithm and a modified system matrix that included the offset between the source and detector locations and the path from the periscope to the source mirror. Figure 9 and Figure 10 show reconstructions at the wavelength bin corresponding to the methane absorption peak along with dashed circle overlays. The outer circle corresponds to the circle of mirrors/detectors while the inner represents the gas plume locations in the system, and the plume location for the reconstruction is in the first position closest to the source mirror.

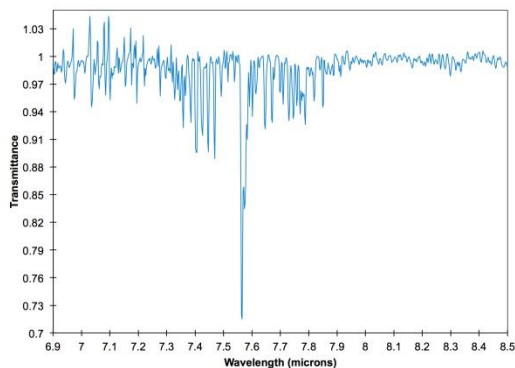


Figure 8. Transmittance plot for Mirror 6 with object placed at position a.

Using the previously described MLE reconstruction modifications, parameters for interpolated pixels between the mirrors and the voxel space mean filter were tested. For both reconstructions shown in Figure 9, interpolation was used to increase projection size from 11 to 111 pixels. No voxel space interpolation was applied in the left reconstruction while a 3 x 3 mean filter in the voxel space was used in the right image. Both reconstructions have concentrations clustered in the correct location for the gas plume location. As seen in the simulated data, interpolation enables reconstruction at a higher sampled voxel space while constraining streak artifacts with large gradients between voxels that are unrealistic for gas distributions. One area poorly sampled in the reconstruction space is between the periscope and the mirror circle; this is because all the paths in this

voxel space lie along a single ray path. The streak in the one o'clock position depicting a high energy corresponds with the poorly sampled periscope location. The use of the mean filter for the reconstruction on the right side of the figure results in a smooth gas distribution with the peak in the correct location.

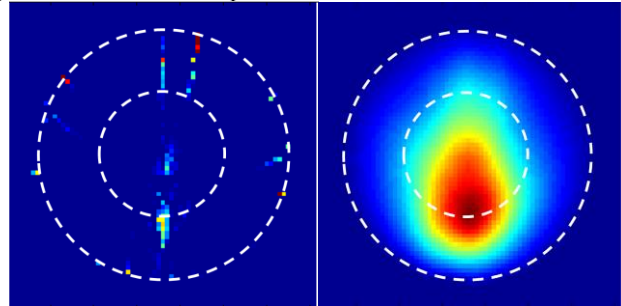


Figure 9. Reconstruction result at 7.656 μm wavelength corresponding to methane absorption peak (left) 10 interpolated pixels with no mean voxel filter (right) 10 interpolated pixels with a 3 x 3 mean voxel filter.

With the lab test data, a third reconstruction was performed with no interpolation between pixels using a 3 x 3 mean filter in the voxel space. This kept the data at 16 projections containing 11 pixels each. This reconstruction is presented in Figure 10. Comparing this reconstruction to the right side of Figure 9 reveals that pixel interpolation in conjunction with the use of a mean filter causes a spatial expansion of the plume area.

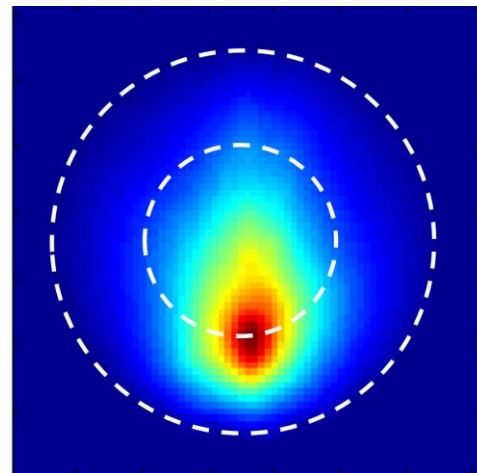


Figure 10. Methane peak reconstruction with no interpolated pixels and 3x3 mean voxel filter.

The reconstruction from Figure 10 was performed for every wavelength bin so that each voxel in the reconstructed plan has an associated spectrum. **Error! Reference source not found.** contains a plot of the spectrum for a voxel located in the plume location and **Error! Reference source not found.** for a voxel outside the plume. Clearly the methane peak is strong at the 7.65 μm wavelength when in the plume location and not when outside of the plume. Additionally, it is evident that absorption at the 7.32 μm wavelength becomes more prominent outside of the methane plume. Additional experimentation is needed to determine which reconstruction configuration is more accurate and to test the system with more than one gas.

Conclusions

An initial proof-of-principle has been performed for a multi-spectral IR-CT system. This includes the acquisition system, using a QCL module for the source, and an iterative reconstruction algorithm based on maximum likelihood expectation. Simulation and laboratory experiments have demonstrated the ability to reconstruct absorption spectra over a spatially distributed space, such that each voxel in the reconstruction has a spectral response that can be further used to identify a gas type and its concentration. The iterative reconstruction algorithm developed for this system uses interpolation in the projection space and mean filtering in the voxel space to force a smooth distribution of a gas in the reconstruction. A quantitative experiment is needed to optimize settings for these parameters and to calibrate reconstructions to quantitative gas concentration values.

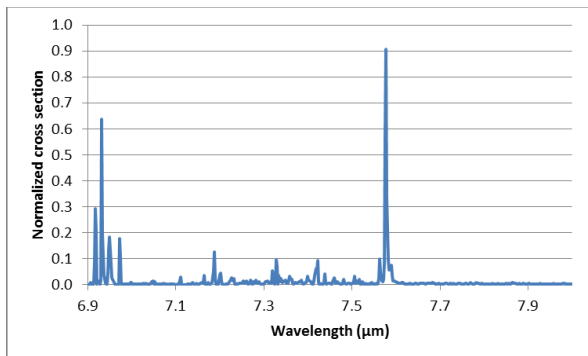


Figure 11. Reconstructed spectrum for voxel in center of reconstructed plume.

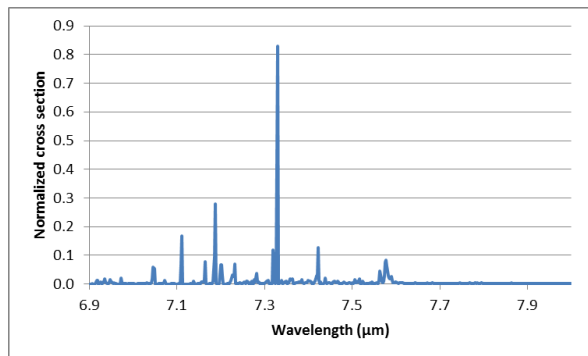


Figure 12. Reconstructed spectrum for voxel outside of plume.

Although not presented in this paper, field experiments were performed with the proof-of-principle system in an outdoor environment with data successfully collected over a test pond. The measurements indicated a 10ppm methane concentration over the pond. Future efforts will need to focus on methods for normalizing measurements in field settings either through additional measurement of known samples for the baseline or use of ratios or differences in the multispectral data to identify specific gasses by their main absorption peaks.

Reprojection of the source around an outdoor-field will require the motion of each mirror in the detector array. Coordination of the motion between the mirrors is the most direct way to produce projections, but this complicates outdoor-field implementation. Follow-on work is needed to develop fieldable control for mirror orientation and investigation of methods that may not require coordinated control of the mirror rotations to ease outdoor-field use.

References

- [1] T. Chowdhury, E. Herndon, T. Phelps, D. Elias, B. Gu, L. Liang, S. Wullschlegel, and D. Graham, Stoichiometry and temperature sensitivity of methanogenesis and CO₂ production from saturated polygonal tundra in Barrow Alaska, *Global Change Biology* 21, 722-737 (2015).
- [2] M. Lara, A. McGuire, E. Euskirchen, C. Tweedie, K. Hinkel, A. Skurikhin, V. Romanovsky, G. Grosse, W. Bolton, and H. Genet, Polygonal tundra geomorphological change in response to warming alters future CO₂ and CH₄ flux on the Barrow Peninsula, *Global Change Biology* 21, 1634-51 (2015).
- [3] D. Zona et al, Cold season emissions dominate the Arctic tundra methane budget, *Proceedings of the National Academy of Sciences of the USA*, 113, 40-45, 2015.
- [4] J. Faist, *Quantum cascade lasers*. (OUP Oxford, 2013).
- [5] C. R. Webster, G. J. Flesch, D. C. Scott, J.E. Swanson, R. D. May, W. S. Woodward, C. Gmachl, F. Capasso, D. L. Sivco, J. N. Baillargeon, A. L. Hutchinson and A. Y. Cho, Quantum-cascade laser measurements of stratospheric methane and nitrous oxide, *Applied Optics* 40, 32 (2001).
- [6] L. Joly, C. Robert, B. Parvitte, V. Catoire, G. Durry, G. Richard, B. Nicoullaud and V. Zéninari., Development of a spectrometer using a continuous wave distributed feedback quantum cascade laser operating at room temperature for the simultaneous analysis of N₂O and CH₄ in the Earth's atmosphere, *Applied Optics* 47, 1206 (2008).
- [7] A. Hartl, B.C. Song, and I. Pundt, 2-D reconstruction of atmospheric concentration peaks from horizontal long path DOAS tomographic measurements: Parametrisation and geometry within a discrete approach, *Atmos. Chem. Phys.* 6, 847-861 (2006)
- [8] M.L. Fischer, P. Price, T. Thatcher, C. Schwalbe, M. Craig, E. Wood, R. Sextro, A. Gadgil, Rapid measurements and mapping of tracer gas concentrations in a large indoor space, *Atmospheric Environment* 3, 2837-44 (2001).
- [9] Greenhouse Gas Laser Imaging Tomography Experiment (Green LITE)
<http://www.netl.doe.gov/File%20Library/factsheets/project/FE0012574.pdf>.
- [10] K. Lange, M. Bahn, and R. Little, A Theoretical Study of Some Maximum Likelihood Algorithms for Emission and Transmission Tomography, *IEEE Transactions on Medical Imaging* Vol. MI-6, No. 2 (1987).
- [11] H. Turbell, New Functionality in take version 2.1, Web material only, Linköping, Sweden, 1999

Author Biography

Philip Bingham received a BS in Electrical and Computer Engineering from the University of Tennessee, and an MS and PhD from the Georgia Institute of Technology. He is currently the group leader for the Imaging, Signals, and Machine Learning Group at Oak Ridge National Laboratory.